We are IntechOpen,
the world's leading publisher of
Open Access books
Built by scientists, for scientists

6,900
Open access books available

186,000
International authors and editors

200M
Downloads

Our authors are among the

154
Countries delivered to

TOP 1%
most cited scientists

12.2%
Contributors from top 500 universities

CLARIVATE ANALYTICS
BOOK CITATION INDEX
INDEXED

WEB OF SCIENCE™

Selection of our books indexed in the Book Citation Index
in Web of Science™ Core Collection (BKCI)

Interested in publishing with us?
Contact book.department@intechopen.com

Multiple-Wavelength Holographic Interferometry with Tunable Laser Diodes

Atsushi Wada
National Defense Academy
Japan

1. Introduction

Two-wavelength holographic interferometry is an effective technique to generate a contour map of a diffusely reflecting surface (Friesem & Levy (1976); Heflinger & Wuerker (1969); Hildebrand & Haines (1967); Yonemura (1985)). In this technique, two holograms are recorded with two wavelengths. An interference fringe pattern is generated by superposing two object images reconstructed from the holograms.

In digital holography, a hologram is recorded by an image sensor and saved into a computer. An object image can be reconstructed by numerical calculation. Several reconstruction methods were reported. Some of these have adjustablity of position and scale of a reconstruction image (Yu & Kim (2006); Zhang et al. (2004)). An object phase distribution can be obtained by the numerical reconstruction of digital holograms. Therefore, two-wavelength digital holographic interferometry makes it possible to generate a contour map by numerical extraction of a phase difference between two reconstructed images (Gass et al. (2003); Parshall & Kim (2006); Wagner et al. (2000; 1999); Yamaguchi (2001); Yamaguchi et al. (2006)). A phase difference extracted from reconstructed object images is wrapped into a half-open interval $(-\pi, \pi]$. If a measured object height was large with respect to a synthetic wavelength, 2π ambiguities of the phase difference should be eliminated for retrieving the object profile. Common phase unwrapping algorithms (Asundi & Wensen (1998); Servin et al. (1998)) which use phase information of neighbor pixels can be applied when an object structure has no discontinuity. However the algorithms can not work correctly for an object profile having isolated region surrounded by discontinuous step.

An object profile with discontinuous structure can be measured by two-wavelength interferometry with a sufficiently large synthetic wavelength. For example, two-wavelength holographic interferometry with a ruby laser and a synthetic wavelength of ~ 2 cm was reported (Heflinger & Wuerker (1969); Pedrini et al. (1999)). Nevertheless the measurement error tends to be amplified linearly with an increase in the synthetic wavelength since most of the error sources are the product of the synthetic wavelength and an error of the extracted phase difference (Cheng & Wyant (1984)).

A technique which eliminates 2π ambiguities by using a phase difference with a large synthetic wavelength was reported (Cheng & Wyant (1985); de Groot (1991); Wagner et al. (2000)). This technique makes it possible to measure a large step-height with high depth resolution. Wagner *et. al.* reported multiple-wavelength holographic interferometry using a dye laser. They combined three phase differences with synthetic wavelengths of 3.04 mm,

1.53 mm and 0.76 mm, and realized the measurement with a measurable step-height of 0.6 mm and an error of 36 μm (Wagner et al. (2000)).

In this paper, multiple-wavelength digital holographic interferometry using tunablity of laser diodes for measuremnt of a large step-height with high accuracy is presented. Using the high-resolution wavelength tunability of laser diodes, a pair of holograms with a small wavelength difference less than 0.01 nm can be recorded, and used to extract a phase difference with a large synthetic wavelength of more than 120 mm. Several holograms are recorded through the change in the wavelength of a laser diode. Phase differences with synthetic wavelengths from 0.4637 mm to 129.1 mm are extracted from the holograms. The synthetic wavelength of 129.1 mm allows us to measure a step-height of 32 mm. The synthetic wavelength of 0.463 mm presents us with a measurement with an rms error of 0.01 mm. 2π ambiguities of the phase difference with a small synthetic wavelength are eliminated by a recursive calculations using the phase difference with a larger synthetic wavelength. The elimination of 2π ambiguities realizes the measurement with the measurable step-height of 32 mm and the rms error of 0.01. The requirements for performing the phase unwrapping are discussed. We found that precise knowledge of the recording wavelengths is required for correctly performing the phase unwrapping. The required precision of the knowledge is derived.

The Fresnel-transform based hologram reconstruction is fast and commonly used. However, the pixel size of reconstructed image increases with the recording wavelength. If the pixel size variation becomes large, the extraction of a phase difference cannot be performed correctly. In order to obtain a correct phase difference, the pixel size should be adjusted. A simple and fast algorithm for pixel size adjustment is described.

2. Hologram recording and reconstruction

Figure 1 shows a geometry of holographic interferometry. A setup for off-axis lensless Fourier transform holography is used for hologram recording. A spherical wave from a point light source is used as a reference wave. An object is located in the same plane as the point light source. A distance between the object and a hologram satisfies the Fresnel approximation (Goodman (1968)). Let the point light source be at $x = 0$, $y = 0$, $z = 0$ and the reference wave $u_{\rm r}(x, y, z)$ is given by

$$u_{\rm r}(x, y, z) = \frac{1}{z} \exp \left(i\pi \frac{x^2 + y^2}{\lambda z} \right), \tag{1}$$

where λ is wavelength.

Let $u_{\rm o}(x, y, z)$ is a complex amplitude of the object light at the hologram. By using a complex amplitude distribution $u_{\rm o}(x', y', 0)$ of the object light in the plane of $z = 0$, $u_{\rm o}(x, y, z)$ is given by

$$u_{\rm o}(x, y, z) = \frac{1}{z} \exp \left(i\pi \frac{x^2 + y^2}{\lambda z} \right) \iint dx' dy' u_{\rm o}(x', y', 0) \exp \left\{ i2\pi \left(\frac{x'^2 + y'^2}{2\lambda z} - \frac{xx' + yy'}{\lambda z} \right) \right\}. \tag{2}$$

We define $u_{\rm o}'$ as the product of $u_{\rm o}(x', y', 0)$ and a spherical wave phase factor, and $U_{\rm o}'$ as the Fourier spectrum of $u_{\rm o}'$:

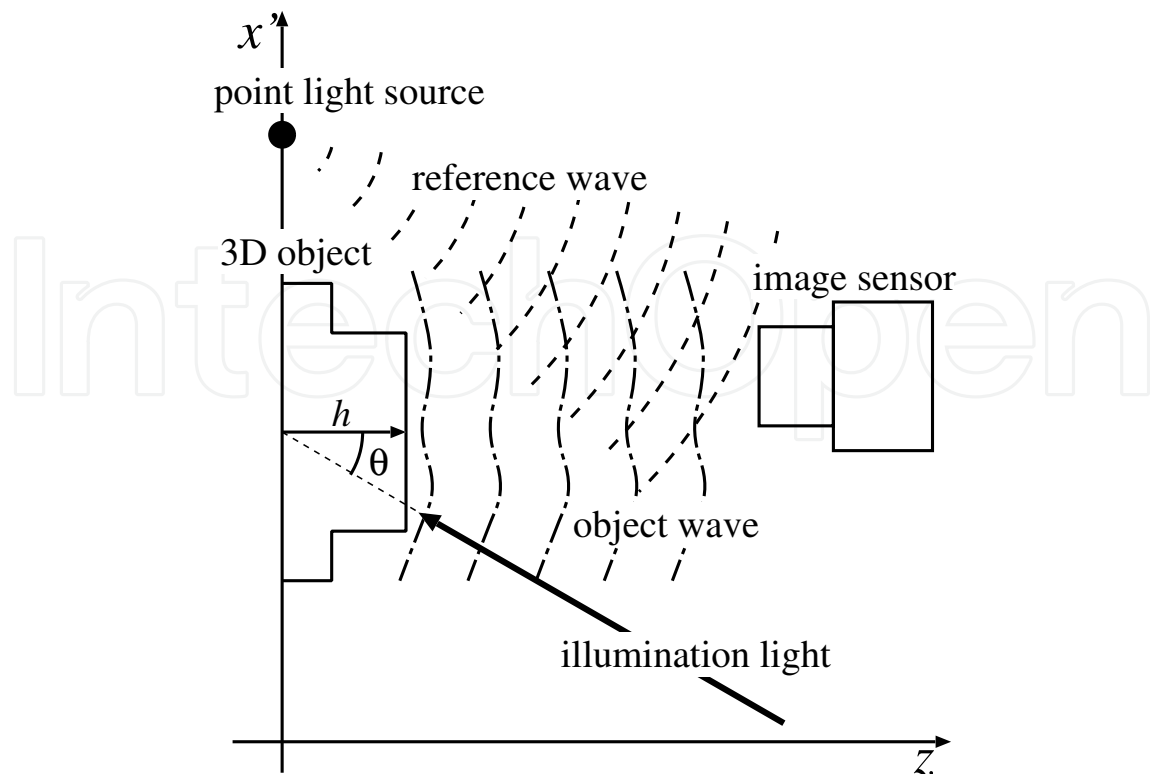$$u_{\rm o}'(x', y') = u_{\rm o}(x', y', 0) \exp \left(i\pi \frac{x'^2 + y'^2}{\lambda z} \right), \tag{3}$$

Fig. 1. Geometry of holographic interferometry.

and

$$U'_o(f'_x, f'_y) = \mathcal{F}(u'_o) = \iint dx'dy' u'_o(x', y') \exp[-i2\pi(f'_x x' + f'_y y')]. \tag{4}$$

Equation (2) can be written in terms of U'_o by substituting the spatial frequencies $f'_x = x/\lambda z$ and $f'_y = y/\lambda z$:

$$u_o(x, y, z) = \frac{1}{z} \exp\left(i\pi\frac{x^2 + y^2}{\lambda z}\right) U'_o\left(\frac{x}{\lambda z}, \frac{y}{\lambda z}\right). \tag{5}$$

An intensity distribution $I(x, y, z)$ of an interference fringe pattern formed by the object wave and the reference wave is given by

$$
\begin{aligned}
I(x, y, z) &= |u_r(x, y, z) + u_o(x, y, z)|^2 \\
&= |u_r|^2 + |u_o|^2 + u_r^* u_o + u_r u_o^* \\
&= \frac{1}{z^2}\left\{1 + \left|U'_o\left(\frac{x}{\lambda z}, \frac{y}{\lambda z}\right)\right|^2 + U'_o\left(\frac{x}{\lambda z}, \frac{y}{\lambda z}\right) + U'^*_o\left(\frac{x}{\lambda z}, \frac{y}{\lambda z}\right)\right\} \\
&= \frac{1}{z^2}\left\{1 + \left|U'_o(f'_x, f'_y)\right|^2 + U'_o(f'_x, f'_y) + U'^*_o(f'_x, f'_y)\right\}.
\end{aligned}
\tag{6}
$$

In Eq. (6), the third term includes the Fourier spectrum of the object light. The object image can be obtained by applying an inverse Fourier transform to $I(x, y, z)$. The reconstructed wave

field u_{rec} obtained by the transformation is given by

$$
\begin{aligned}
u_{\text{rec}}(x',y') &= \mathcal{F}^{-1}\{I(x,y,z)\} \\
&= \mathcal{F}^{-1}\{I(\lambda z f_x', \lambda z f_y', z)\} \\
&= \iint df_x' df_y' \, I(\lambda z f_x', \lambda z f_y', z) \exp[i2\pi(f_x' x' + f_y' y')] \\
&= \lambda^2 \left\{ \frac{\delta(x',y')}{\lambda^2 z^2} + u_o'(x',y') \otimes u_o'^*(-x',-y') + u_o'(x',y') + u_o'^*(-x',-y') \right\},
\end{aligned}
\tag{7}
$$

where the symbol $\otimes$ stands for the convolution operator. In Eq. (7), the first term is the reference point light source. The second term is an autocorrelation of the object light. The third term expresses the object light produced by a spherical wave phase factor. The fourth term is the complex conjugate of the third term. Since a phase factor does not affect intensity, the intensity distribution of the object light can be reconstructed by the third term of Eq. (7). Let consider that $I(x,y,z)$ is recorded by an image sensor having $N_x \times N_y$ pixels with pixel size of $\Delta_x \times \Delta_y$. Numerical reconstruction of the digital hologram is realized through the inverse discrete Fourier transform. Let the pixel size of the numerically reconstructed object image be $\Delta_x' \times \Delta_y'$. The discrete formulation of Eq. (7) is then

$$
u_{\text{rec}}(s\Delta_x', t\Delta_y') = \sum_{p=-N_x/2}^{N_x/2-1} \sum_{q=-N_y/2}^{N_y/2-1} I(p\Delta_x, q\Delta_y, z) \exp\left\{ i2\pi \left(\frac{p\Delta_x}{\lambda z} s\Delta_x' + \frac{q\Delta_y}{\lambda z} t\Delta_y' \right) \right\},
\tag{8}
$$

where p, q are integers, and s, t are integers and fulfill $x' = s\Delta_x'$, $y' = t\Delta_y'$. The right side of Eq. (8) is arranged in the form, in which fast Fourier transform can be applied:

$$
u_{\text{rec}}(s\Delta_x', t\Delta_y') = \sum_{p=-N_x/2}^{N_x/2-1} \sum_{q=-N_y/2}^{N_y/2-1} I(p\Delta_x, q\Delta_y, z) \exp\left\{ i2\pi \left(\frac{ps}{N_x} + \frac{qt}{N_y} \right) \right\},
\tag{9}
$$

where s, t, p and q are integers, and Δ_x', Δ_y' satisfy the following condition

$$
\Delta_x' = \frac{\lambda z}{\Delta_x N_x}, \; \Delta_y' = \frac{\lambda z}{\Delta_y N_y},
\tag{10}
$$

and

$$
-N_x/2 \leq s < N_x/2, \; -N_y/2 \leq t < N_y/2.
\tag{11}
$$

The field of view of the reconstructed image is $\lambda z / \Delta_x \times \lambda z / \Delta_y$.

3. Multiple-wavelength interferometry

The reference plane is assumed to be placed at $z = 0$. Let the illumination light irradiate to the object at an angle θ to the reference plane, and the height of the object surface respect to the reference plane be $h(x',y')$. The phase distribution $\phi(x',y')$ of the reconstructed image is given by

$$
\phi(x',y') = \frac{2\pi}{\lambda} \left\{ -L + \frac{x'^2 + y'^2}{2z} \right\},
\tag{12}
$$

where L is an optical path difference caused by the object surface structure, giving

$$L = (1 + \cos\theta)h(x', y') - x'\sin\theta. \tag{13}$$

The second term of Eq. (12) is the spherical wavefront introduced in Eq. (3).

Holograms are recorded with wavelengths of λ_n satisfying $\lambda_n < \lambda_{n+1}$ and the phase distribution of the object wave at the plane of $z = 0$ is ϕ_n. The phase difference $\Delta\phi_n$ between ϕ_n and ϕ_0 is given by

$$\Delta\phi_n(x', y') = \phi_n - \phi_0 = \frac{2\pi}{\Lambda_n}\left(L + \frac{x'^2 + y'^2}{2z}\right) \simeq \frac{2\pi}{\Lambda_n}L, \tag{14}$$

where Λ_n are synthetic wavelengths and

$$\Lambda_n = \frac{\lambda_0\lambda_n}{\lambda_n - \lambda_0} \simeq \frac{\bar{\lambda}_n^2}{\Delta\lambda_n}, \tag{15}$$

where $\bar{\lambda}_n$ and $\Delta\lambda_n$ are the average and difference of wavelengths given by

$$\bar{\lambda}_n = \frac{\lambda_0 + \lambda_n}{2}, \ \Delta\lambda_n = \lambda_n - \lambda_0. \tag{16}$$

In Eq. (8), the condition $z \gg (x'^2 + y'^2)/\Lambda_n$ is assumed and a quadratic phase term is neglected.

Let Ψ_n be the phase difference extracted from the image reconstructed from the hologram with wavelength of λ_n. The phase difference Ψ_n are given by

$$\Psi_n = \tan^{-1}\frac{\text{Im}(u'_{on}u'_{o0}{}^*)}{\text{Re}(u'_{on}u'_{o0}{}^*)}. \tag{17}$$

Ψ_n is wrapped into $(-\pi, \pi]$ and the relation between Ψ_n and $\Delta\phi_n$ is given by

$$\Delta\phi_n = \Psi_n + 2\pi m_n, \tag{18}$$

where m_n is an integer. If the conditions of $\Delta\phi_1 = \Psi_1$ and $\Lambda_n < \Lambda_{n-1}$ are satisfied, $\Delta\phi_n$ can be retrieved (Nadeborn et al. (1996); Paulsson et al. (2000); Wagner et al. (2000)) through recursive calculation of

$$\Delta\phi_n = \Psi_n + 2\pi\text{NINT}\left(\frac{\alpha_n\Delta\phi_{n-1} - \Psi_n}{2\pi}\right), \tag{19}$$

where $\text{NINT}(a)$ denotes the function returning the nearest neighbor integer of argument a, and α_n is the sensitivity ratio between each phase difference $\Delta\phi_n$ and $\Delta\phi_{n-1}$ and given by

$$\alpha_n = \frac{\Lambda_{n-1}}{\Lambda_n}. \tag{20}$$

4. Requirements for the phase unwrapping

In this section, we discuss the requirements for correctly performing the phase unwrapping. First, the requirements of the measurement error and the sensitivity ratio between the phase differences are discussed based on the assumption that the error of the sensitivity ratio is negligible small. Next, it is pointed out that the sensitivity ratio should be estimated for the phase unwrapping. Then, the required accuracy of the sensitivity ratio is derived. Lastly, it is explained how precise measurement of the wavelengths is required for high accuracy estimation of the sensitivity ratio.

Let the true phase differences and the sensitivity ratio are defined as $\Delta\phi'_n$, Ψ'_n and α'_n, and the measurement errors of the phase differences and the sensitivity ratio are defined as $\Psi_{\epsilon,n}$ and $\alpha_{\epsilon,n}$. The relations between these parameters and Ψ, $\Delta\phi$ and α are given by

$$\Psi_n = \Psi'_n + \Psi_{\epsilon,n}, \ \Delta\phi'_n = \Psi'_n + 2\pi m_n = \Delta\phi_n - \Psi_{\epsilon,n}, \ \alpha_n = \alpha'_n + \alpha_{\epsilon,n}. \tag{21}$$

By substituting Eqs. (21) into Eq. (19), we get

$$\Delta\phi_n = \Psi'_n + \Psi_{\epsilon,n} + 2\pi\mathrm{NINT}\left(\frac{(\alpha'_n + \alpha_{\epsilon,n})(\Delta\phi'_{n-1} + \Psi_{\epsilon,n-1}) - \Psi'_n - \Psi_{\epsilon,n}}{2\pi}\right). \tag{22}$$

For the true phase difference and sensitivity ratio, the condition

$$\frac{\alpha'_n\Delta\phi'_{n-1} - \Psi'_n}{2\pi} = \frac{\Delta\phi'_n - \Psi'_n}{2\pi} = m_n, \tag{23}$$

is satisfied. Substituting Eqs. (23) into Eq. (22) gives

$$\Delta\phi_n = \Delta\phi'_n + \Psi_{\epsilon,n} + 2\pi\mathrm{NINT}\left(\frac{\alpha_{\epsilon,n}(\Delta\phi'_{n-1} + \Psi_{\epsilon,n-1}) + \alpha_n\Psi_{\epsilon,n-1} - \Psi_{\epsilon,n}}{2\pi}\right). \tag{24}$$

In order to correctly perform the phase unwrapping, the third term in the right side of Eq. (24) should be zero, and the condition

$$\left|\frac{\alpha_{\epsilon,n}\Delta\phi'_{n-1} + \alpha_n\Psi_{\epsilon,n-1} - \Psi_{\epsilon,n}}{2\pi}\right| < \frac{1}{2}, \tag{25}$$

should be satisfied. In Eq. (25), the condition $\Psi_{\epsilon,n-1} \ll \Delta\phi'_{n-1}$ is assumed. Let the maximum of $|\Psi_{\epsilon,n}|$ for all n be $2\pi\epsilon$:

$$|\Psi_{\epsilon,n}| \le 2\pi\epsilon. \tag{26}$$

Let the true synthetic wavelength be defined as Λ'_n. Substituting $\Delta\phi'_{n-1}$, α'_n and Λ'_n into Eq. (8) gives

$$\Delta\phi'_{n-1} = \frac{2\pi L}{\alpha'_n\Lambda'_n}. \tag{27}$$

Substitution of Eqs. (26) and (27) into Eq. (25) gives

$$\epsilon < \frac{1}{\alpha'_n + 1}\left(\frac{1}{2} - \frac{|\alpha_{\epsilon,n}|}{\alpha'_n}\frac{L}{\Lambda'_n}\right). \tag{28}$$

If the assumption $|\alpha_{\epsilon,n}| \ll \alpha'_n$ is introduced, we have the requirements

$$\epsilon < \frac{1}{2(\alpha'_n + 1)}, \tag{29}$$

and

$$\alpha'_n < \frac{1 - 2\epsilon}{2\epsilon}. \tag{30}$$

The requirements of ϵ and α'_n seem to be relaxed as compared with the requirements derived in previous works (Nadeborn et al. (1996); Wagner et al. (2000)). For example, if $\alpha'_n = 2$ then the upper limit of ϵ is $1/6$. In other words, if $\epsilon = 1/12$ then the upper limit of α'_n is 5. It should be noted that the requirements denoted in Eqs. (29) and (30) are based on the assumption of $|\alpha_{\epsilon,n}| \ll \alpha'_n$. If there has been a small error of the phase difference sensitivity ratio such as $|\alpha_{\epsilon,n}|/\alpha'_n = 1/40$, the upper limit of ϵ and α'_n become small to $1/12$ and 2 respectively with $\Lambda'_n = 2.5$ mm and $L = 25$ mm.

Let us consider how accurate an estimation of the phase difference sensitivity ratio is required for the phase unwrapping. By solving Eq. (28) for $|\alpha_{\epsilon,n}|$, we obtain the condition

$$|\alpha_{\epsilon,n}| < \alpha'_n \frac{\Lambda'_n}{L} \left(\frac{1}{2} - \epsilon(\alpha'_n + 1) \right). \tag{31}$$

This shows that the upper limit of the measurement error of the sensitivity ratio for correctly performing the phase unwrapping become small in proportion to $\alpha'_n \Lambda'_n / L$. This means that α_n should be precisely estimated for measuring a large object height by using a small synthetic wavelength. For example, if $\alpha'_n = 2$, $\Lambda'_n = 2.5$ mm, $L = 25$ mm and $\epsilon = 1/12$, then $|\alpha_{\epsilon,n}|$ should be less than $1/20$.

Let us consider how precise the measurement of the wavelengths is required to be for the phase unwrapping. Let the true value of wavelength be λ'_n, and the true and the measurement error of the wavelength difference are defined as $\Delta\lambda'_n$ and $\Delta\lambda_{\epsilon,n}$. By calculating the error propagation of $\Delta\lambda_n$ in Eq. (15), we have

$$\frac{\alpha_{\epsilon,n}}{\alpha'_n} \frac{L}{\Lambda'_n} = \left(\frac{\Delta\lambda_{\epsilon,n-1}}{\Delta\lambda'_{n-1}} - \frac{\Delta\lambda_{\epsilon,n}}{\Delta\lambda'_n} \right) \frac{L\Delta\lambda'_n}{\bar{\lambda}_n^2}. \tag{32}$$

Let the maximum of $|\Delta\lambda_{\epsilon,n}|$ for all n be $\Delta\lambda_\epsilon$:

$$|\Delta\lambda_{\epsilon,n}| \leq \Delta\lambda_\epsilon. \tag{33}$$

By substituting Eqs. (32) and (33) into Eq. (28) and solving for $\Delta\lambda_\epsilon$, we obtain the condition

$$\Delta\lambda_\epsilon < \frac{\bar{\lambda}_n^2}{L} \left(\frac{1}{2(\alpha'_n + 1)} - \epsilon \right). \tag{34}$$

For example, $\alpha'_n = 2$, $\bar{\lambda}_n = 800$ nm, $L = 25$ mm, and $\epsilon = 1/12$, $\Delta\lambda_\epsilon$ should be less than 0.002 nm.

5. Scale adjustment for phase calculation

In the Fresnel-transform based method (FTM), the pixel size of the reconstructed image increases with the reconstruction distance and the recording wavenumber. The variation of the pixel size poses problems in holographic interferometry (Yamaguchi et al. (2006)). In contrast, the convolution method (CM) (Yamaguchi et al. (2002)) keeps the pixel size of the reconstructed image the same as the pixel size of an image sensor used for hologram recording. However, the CM requires huge computational time with respect to the FTM. A

zero padding method was proposed to control the pixel size of the image reconstructed by the FTM (ALFIERI et al. (2006); Ferraro et al. (2004)). In this method, an increase in the total pixel number of the hologram decreases the pixel size of the reconstructed image and can cause an explosive increase of the computational time as a result of the impossibility of the fast Fourier transform (FFT) application in the reconstruction. Algorithms based on an approach of splitting the reconstruction process into two diffraction processes were reported (Yu & Kim (2006); Zhang et al. (2004)). The methods require almost the twice computational time with respect to the FTM.

We present a simple and fast adjustment of pixel size in the reconstructed image. We adjust the pixel size by magnifying a recorded hologram before reconstruction of the hologram. The total pixel number of the hologram can be maintained for the possibility of the FFT application. Only one time calculation of the diffraction is required. Let consider that a hologram is recorded with the wavelength of λ_1, and an another hologram is recorded with the wavelength of λ_2. By application of a image magnification into the second hologram plane, the pixel sizes of the images reconstructed from the holograms are adjusted to be the same. Let the rescaled pixel size of the second hologram in a hologram plane be $\Delta_{x2} \times \Delta_{y2}$. For the adjustment, Δ_{x2} and Δ_{y2} should satisfy

$$\Delta_{x2} = \Delta_x \frac{\lambda_2}{\lambda_1}, \ \Delta_{y2} = \Delta_y \frac{\lambda_2}{\lambda_1}. \tag{35}$$

Experiments are performed to demonstrate the effectiveness of our pixel adjustment method. A test object was a Japanese one yen coin. Intensity and phase distributions of an image reconstructed from a hologram are shown in Fig. 2. As shown in Fig. 2 (b), the phase distribution has a random structure due to the light scattering from the diffusely surface of the object.

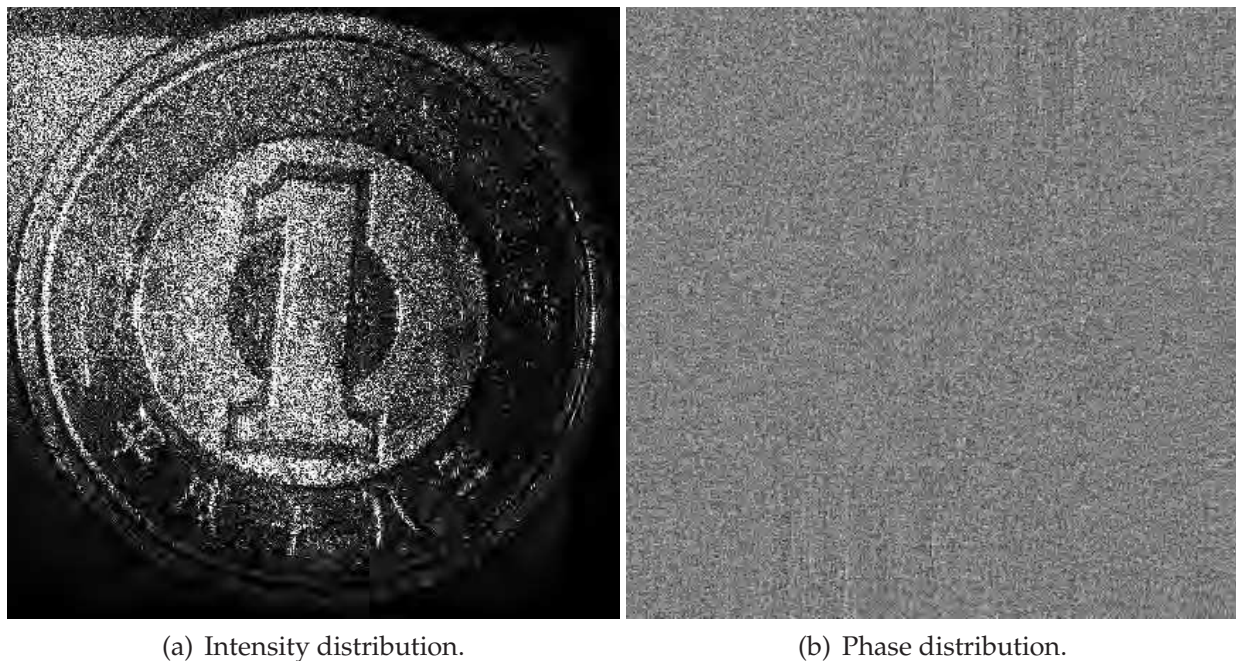| (a) Intensity distribution. | (b) Phase distribution. |

Fig. 2. Reconstructed image of hologram.

Holograms were recorded through changing the wavelength by injection current control of the laser diode. Three holograms with the recording wavelengths of 783.39 nm , 783.59 nm

and 785.14 nm were used for two-wavelength holographic interferometry. Figure 3 shows the phase differences extracted from the images reconstructed from the holograms using no scale adjustment. As shown in Fig. 3 (a), it is clear that the phase subtraction was correctly performed on the entire object with the wavelength difference of 0.20 nm. In contrast, the phase difference with the wavelength difference of 1.75 nm shown in Fig. 3 (b) has random structures in the right and the lower side. The random structures were caused by incorrect phase subtraction due to the changes in the pixel size of the reconstructed image.

(a) $\Delta\lambda = 0,20\,\mathrm{nm}$ (b) $\Delta\lambda = 1.75\,\mathrm{nm}$

Fig. 3. Phase difference distributions calculated using no scale adjustment.

The present method was applied to solve the problem in the phase subtraction for two-wavelength holographic interferometry. The bilinear interpolation (Kreis (2005)) was used for image magnification. Figure 4 show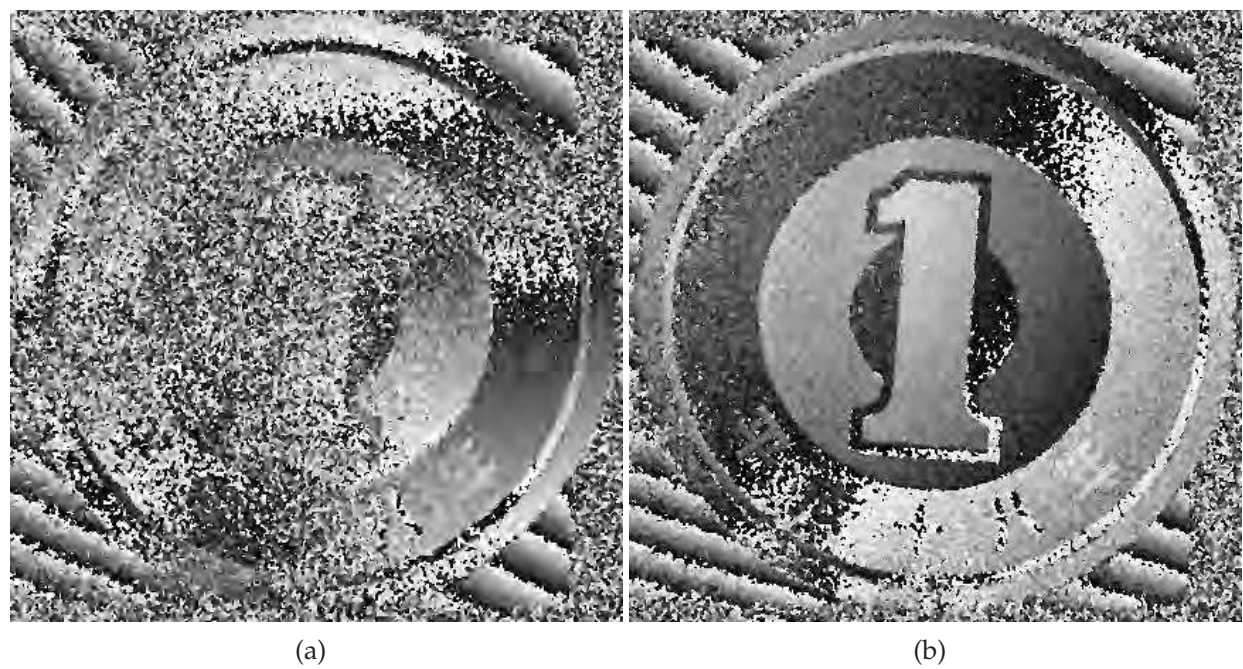s phase difference distributions with a wavelength difference of 1.75 nm calculated using scale adjustment by application of the bilinear interpolation after and before reconstruction of the hologram. It is seen that a random structure appears on a part of the phase difference shown in Fig. 4 (a). As shown in Fig. 4 (b), it is clear that the phase subtraction was correctly performed on the entire object. This means that the present method completely solved the problem in the phase subtraction due to the changes in the pixel size.

6. Experiment

Figure 5 shows an optical setup for hologram recording. The light source was a laser diode (Hitachi HL7851G) with a wavelength of 785 nm and an output power of 50 mW. The image sensor was a CCD camera (Prosilica EC1350) having pixels of 1360×1024 with a pitch of 4.65 μm $\times$ 4.65 μm.

A beam emitted from the laser diode was collimated by a objective lens OL1 and then cleaned by a objective lens OL2 and a pinhole. The beam was again collimated by a lens L1 and separated into two beams by a half mirror. One was expanded by lenses L2 and L3 and reflected by a half mirror to illuminate the object. The angle of incidence θ was equal to zero.

<div align="center">(a)   (b)</div>

Fig. 4. Phase difference distributions with a wavelength difference of 1.75 nm calculated using scale adjustment by application of the bilinear interpolation (a) after- and (b) before-reconstruction of the hologram.
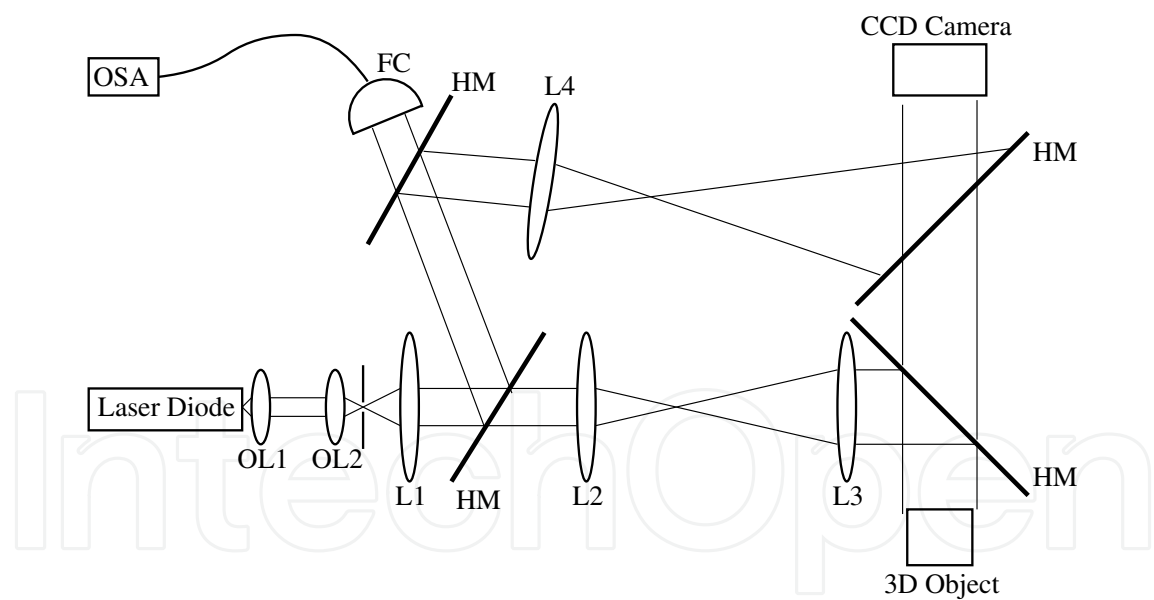

Fig. 5. Hologram recording setup. OSA: optical spectrum analyzer; FC: fiber coupler; HM: half mirror; OL1: $\times$ 10 objective lens; OL2: 5 $\times$ objective lens; L1: lens (f =60 mm); L2: lens (f=70 mm); L3: lens (f=170 mm); L4: lens (f=60 mm).

The other beam was again splited by a half mirror. The light transmitted through the half mirror was coupled into a fiber coupler and detected by an optical spectrum analyzer. The light reflected by the half mirror was focused by a lens L4 and became a reference point light source.
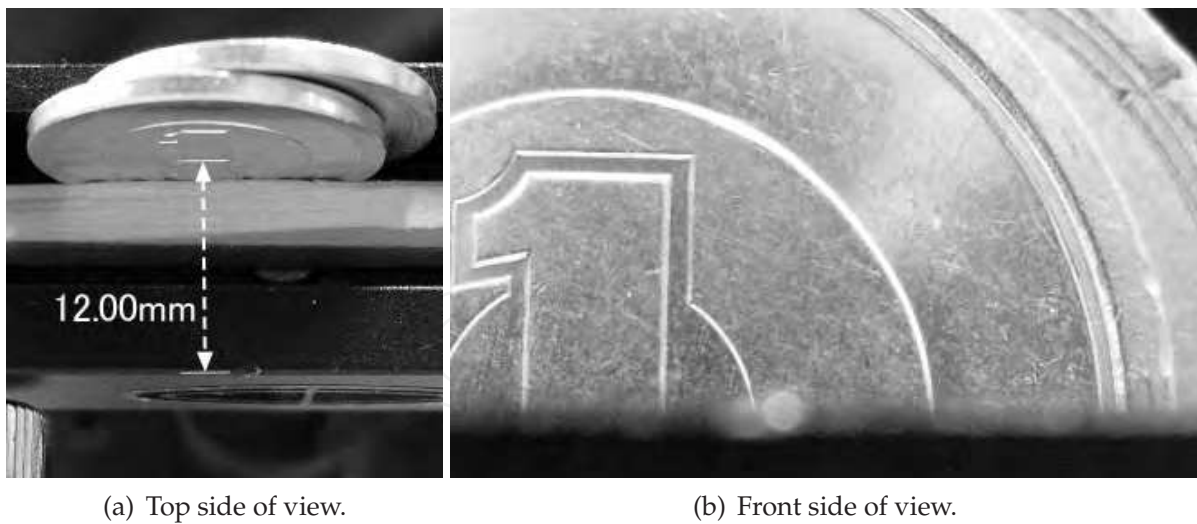
(a) Top side of view.   (b) Front side of view.

Fig. 6. Photograph of a test object.

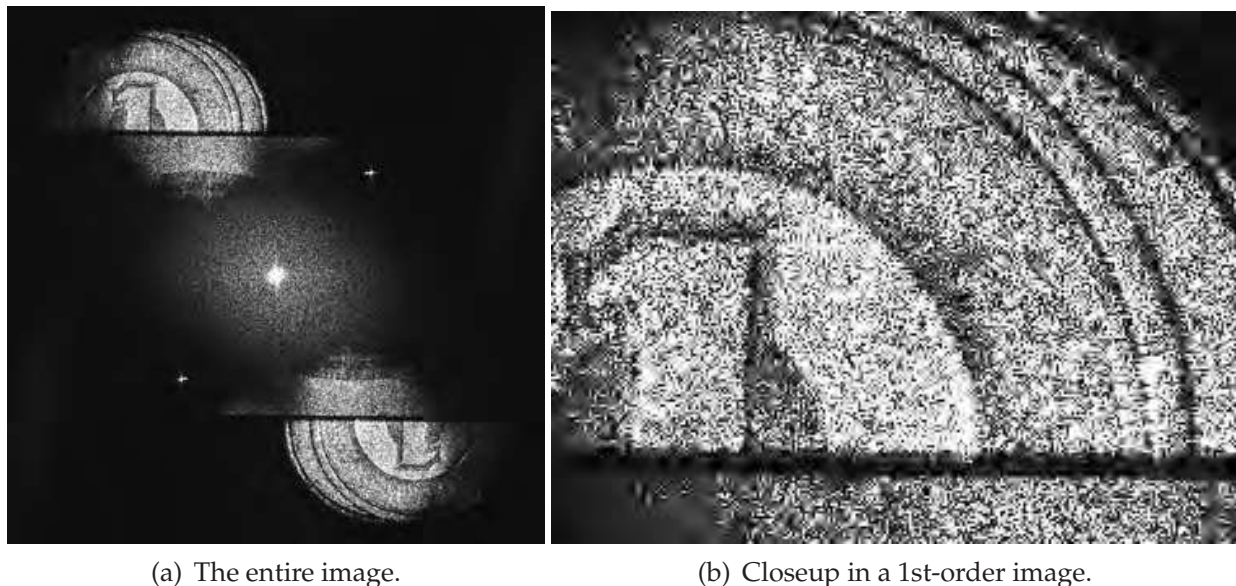(a) The entire image.   (b) Closeup in a 1st-order image.

Fig. 7. Image reconstructed from a hologram.

The distance between the object and the camera was 300 mm. The field of view of a reconstructed object image was 50 mm × 50 mm. As shown in Fig.6, a test object was a Japanese one yen coin.

For keeping an aspect ratio of a reconstructed object image equal to 1.0, the central region with 1024 × 1024 pixels of a hologram was used for the object image reconstruction.

The reconstructed image is shown in Fig. 7. The object light and its conjugate were reconstructed at the upper left and the lower right. Two bright points in the upper right and the lower left are produced by reflection at the back surface of a half mirror.

Holograms were recorded through changing the wavelength of a laser diode by injection current and operation temperature controls. The power spectral distribution of the laser light was measured using an optical spectrum analyzer(Ando Electric AQ-63515A) during hologram recording. The specification of the analyzer was as follows: the wavelength accuracy was 0.05 nm, the resolution was 0.05 nm, and the repeatability was 0.005 nm.

(a) Ψ_1 (b) Ψ_2 (c) Ψ_3

(d) Ψ_4 (e) Ψ_5 (f) Ψ_6

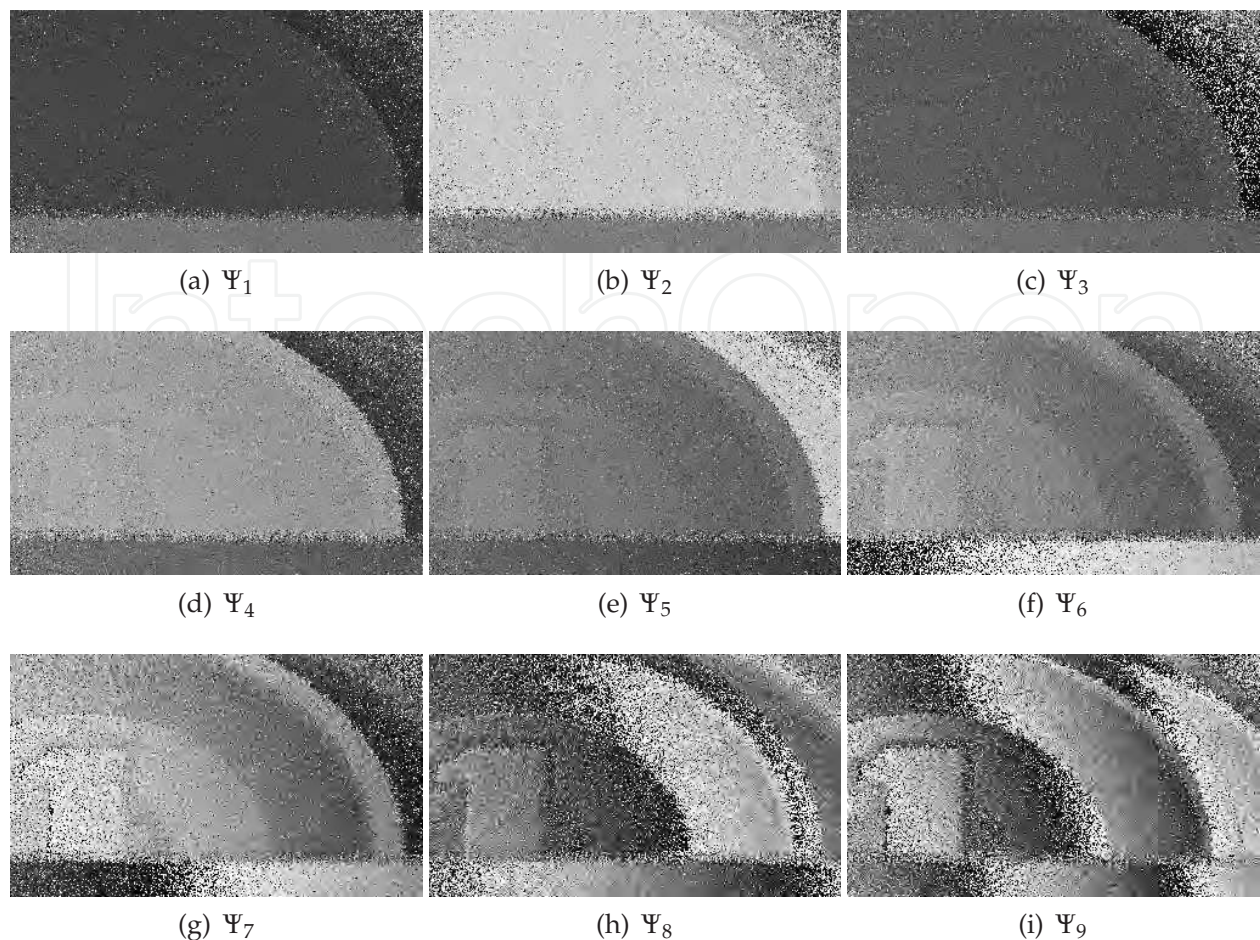(g) Ψ_7 (h) Ψ_8 (i) Ψ_9

Fig. 8. Phase differences.

The central wavelength was obtained through the calculation of the center of gravity in the spectrum distribution measured using the optical spectrum analyzer.

Ten holograms for phase difference extraction were chosen from the holograms. The phase differences Ψ_n were extracted from the object images reconstructed from the holograms with wavelengths λ_n. Figure 8 shows Ψ_n. It can be seen in Fig. 8 that the phase differences have a salt-and-pepper noize produced by speckle noize. As shown in later, the noize can be suppressed by image processing method such as smoothing and median filtering (Yamaguchi (2001); Yamaguchi et al. (2006)).

The unwrapped phase differences $\Delta\phi_n$ were retrieved by the recursive calculations of Eq. (19). The synthetic wavelengths were calibrated (Wada et al. (2008)) by the comparison between the phase differences and the object height measured by using a slide caliper. The calibrated synthetic wavelengths were $\Lambda_1 = 129.1$mm, $\Lambda_2 = 34.02$mm, $\Lambda_3 = 11.47$mm, $\Lambda_4 = 8.593$mm, $\Lambda_5 = 4.914$mm, $\Lambda_6 = 2.849$mm, $\Lambda_7 = 1.380$mm, $\Lambda_8 = 0.9061$mm, $\Lambda_9 = 0.4637$mm.

The object profile was obtained using $\Delta\phi_n$. Since the incident angle θ for the object illumination was equal to zero, $L = 2h$ and

$$h = \frac{\Lambda_n \Delta\phi_n}{4\pi}. \tag{36}$$

Because $\Delta\phi_1 = \Psi_1$ and a phase difference within $(-\pi, \pi]$ corresponds to a object height within $(-\Lambda_n/4, \Lambda_n/4]$, a measurable step height is $\Lambda_1/4$ = 32 mm. The object height distributions

calculated by $\Delta\phi_n$ with Λ_n are shown in Fig. 9. Figure 10 shows the plot of the object heights along a line denoted in white and black in Fig. 9 (i) as a function of the lateral positions. Figure 10 shows that the step-heights of 0.1 mm and 12 mm were correctly detected.
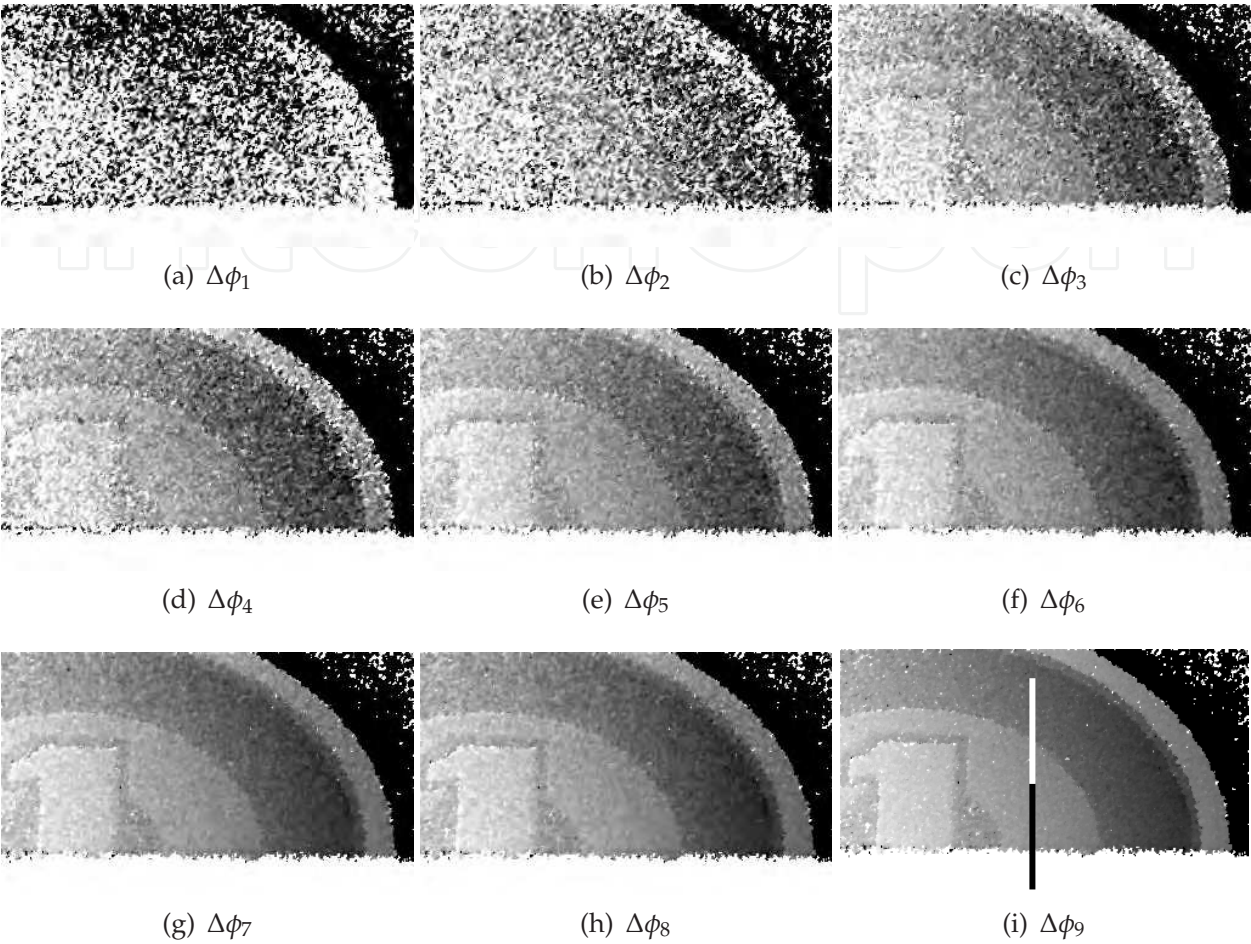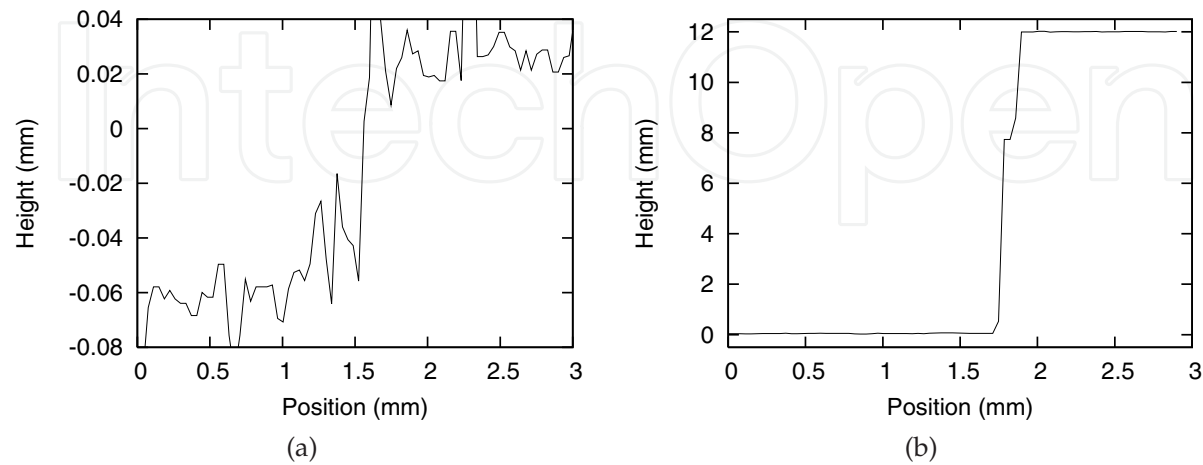

(a) $\Delta\phi_1$ (b) $\Delta\phi_2$ (c) $\Delta\phi_3$

(d) $\Delta\phi_4$ (e) $\Delta\phi_5$ (f) $\Delta\phi_6$

(g) $\Delta\phi_7$ (h) $\Delta\phi_8$ (i) $\Delta\phi_9$

Fig. 9. An object height calculated from $\Delta\phi_n$

(a)   (b)

Fig. 10. Plot of the object heights along a line denoted in (a) white and (b) black in Fig.9 (i) as a function of lateral positions.
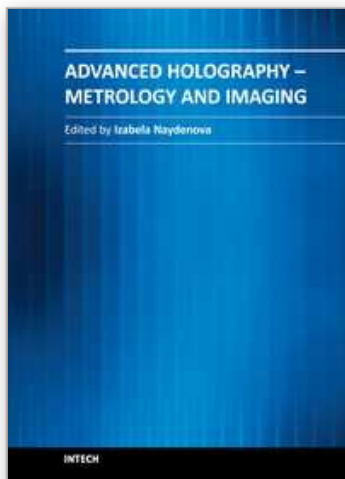
7. Conclusion

Multiple-wavelength digital holographic interferometry using tunablity of laser diodes for measuring a large step-height with high accuracy was presented. The requirements for performing the phase unwrapping were discussed. We have found that precise knowledge of the recording wavelengths is required for correctly performing the phase unwrapping. The required precision of the knowledge was derived. A simple and fast algorithm for pixel size adjustment was presented. It has been demonstrated that the problem of the phase subtraction in two-wavelength holographic interferometry can be solved by the present method.

Several holograms were recorded through the changes in the wavelength of a laser diode by injection current and operation temperature controls. A pair of holograms with a small wavelength difference less than 0.01 nm was recorded and used for realizing holographic interferometry with a large synthetic wavelength more than 120 mm. Phase differences with synthetic wavelengths from 0.4637 mm to 129.1 mm were extracted by using the holograms. The synthetic wavelengths were calibrated by the comparison between the phase differences and the object heights measured by using a slide caliper. The step-heights of 0.1 mm and 12 mm were correctly detected.

8. References

Alfieri, D., Coppola, G., Denicola, S., Ferraro, P., Finizio, A., Pierattini, G. & Javidi, B. (2006). Method for superposing reconstructed images from digital holograms of the same object recorded at different distance and wavelength, *Optics Communications* 260(1): 113–116.
URL: *http://dx.doi.org/10.1016/j.optcom.2005.10.055*

Asundi, A. & Wensen, Z. (1998). Fast Phase-Unwrapping Algorithm Based on a Gray-Scale Mask and Flood Fill, *Applied Optics* 37(23): 5416.
URL: *http://ao.osa.org/abstract.cfm?URI=ao-37-23-5416*

Cheng, Y.-Y. & Wyant, J. C. (1984). Two-wavelength phase shifting interferometry, *Applied Optics* 23(24): 4539.
URL: *http://ao.osa.org/abstract.cfm?URI=ao-23-24-4539*

Cheng, Y.-Y. & Wyant, J. C. (1985). Multiple-wavelength phase-shifting interferometry, *Applied Optics* 24(6): 804.
URL: *http://ao.osa.org/abstract.cfm?URI=ao-24-6-804*

de Groot, P. (1991). Three-color laser-diode interferometer, *Applied Optics* 30(25): 3612.
URL: *http://ao.osa.org/abstract.cfm?URI=ao-30-25-3612*

Ferraro, P., De Nicola, S., Coppola, G., Finizio, A., Alfieri, D. & Pierattini, G. (2004). Controlling image size as a function of distance and wavelength in Fresnel-transform reconstruction of digital holograms, *Optics Letters* 29(8): 854.
URL: *http://ol.osa.org/abstract.cfm?URI=ol-29-8-854*

Friesem, A. A. & Levy, U. (1976). Fringe formation in two-wavelength contour holography, *Applied Optics* 15: 3009–3020.
URL: *http://ao.osa.org/abstract.cfm?id=20668*

Gass, J., Dakoff, A. & Kim, M. K. (2003). Phase imaging without 2π ambiguity by multiwavelength digital holography, *Optics Letters* 28(13): 1141–1143.
URL: *http://www.opticsinfobase.org/abstract.cfm?URI=ol-28-13-1141*

Goodman, J. W. (1968). *Introduction to Fourier Optics*, McGraw-Hill, New York.

Heflinger, L. O. & Wuerker, R. F. (1969). Holographic Contouring Via Multifrequency Lasers, *Applied Physics Letters* 15: 28.
URL: *http://scitation.aip.org/getabs/servlet/GetabsServlet?prog=normal&id=APPLAB0000 15000001000028000001&idtype=cvips&gifs=yes*

Hildebrand, B. P. & Haines, K. A. (1967). Multiple-wavelength and multiple-source holography applied to contour generation, *Journal of the Optical Society of America* 57: 155–162.
URL: *http://www.opticsinfobase.org/abstract.cfm?id=75509*

Kreis, T. (2005). *Handbook of holographic interferometry: optical and digital methods*, Wiley-VCH.
URL: *http://books.google.com/books?id=H5nO1i7CR8cC&pgis=1*

Nadeborn, W., Andrä, P. & Osten, W. (1996). A Robust Procedure for Absolute Phase Measurement, *Optics and Lasers in Engineering* 24(2): 245–260.
URL: *http://www.sciencedirect.com/science?_ob=GatewayURL&_origin=ScienceSearch& _method=citationSearch&_piikey=0143816695000178&_version=1&_returnURL=&md5= 91f687b89ebc9a690103a69e85082d62*

Parshall, D. & Kim, M. K. (2006). Digital holographic microscopy with dual-wavelength phase unwrapping, *Applied Optics* 45(3): 451–459.
URL: *http://www.ncbi.nlm.nih.gov/entrez/query.fcgi?cmd=Retrieve&db=pubmed&dopt= Abstract&list_uids=16463728*

Paulsson, L., Sjdahl, M., Kato, J. & Yamaguchi, I. (2000). Temporal Phase Unwrapping Applied to Wavelength-Scanning Interferometry, *Applied Optics* 39(19): 3285–3288.
URL: *http://ao.osa.org/abstract.cfm?customerkey=422ab3c3-851b-405f-9df2-adcd7de575fb &id=62589*

Pedrini, G., Fröning, P., Tiziani, H. J. & Gusev, M. E. (1999). Pulsed digital holography for high-speed contouring that uses a two-wavelength method, *Applied Optics* 38: 3460–3467.
URL: *http://www.opticsinfobase.org/abstract.cfm?id=44295*

Servin, M., Marroquin, J. L., Malacara, D. & Cuevas, F. J. (1998). Phase Unwrapping with a Regularized Phase-Tracking System, *Applied Optics* 37(10): 1917.
URL: *http://ao.osa.org/abstract.cfm?URI=ao-37-10-1917*

Wada, A., Kato, M. & Ishii, Y. (2008). Multiple-wavelength digital holographic interferometry using tunable laser diodes, *Applied Optics* 47(12): 2053.
URL: *http://ao.osa.org/abstract.cfm?URI=ao-47-12-2053*

Wagner, C., Osten, W. & Seebacher, S. (2000). Direct shape measurement by digital wavefront reconstruction and multiwavelength contouring, *Optical Engineering* 39: 79–85.
URL: *http://spiedl.aip.org/getabs/servlet/GetabsServlet?prog=normal&id=OPEGAR000039 0000001000079000001&idtype=cvips&gifs=yes*

Wagner, C., Seebacher, S., Osten, W. & Jüptner, W. (1999). Digital Recording and Numerical Reconstruction of Lensless Fourier Holograms in Optical Metrology, *Applied Optics* 38: 4812–4820.
URL: *http://ao.osa.org/abstract.cfm?id=44347*

Yamaguchi, I. (2001). Surface contouring by phase-shifting digital holography, *Optics and Lasers in Engineering* 36(5): 417–428.
URL: *http://dx.doi.org/10.1016/S0143-8166(01)00069-0*

Yamaguchi, I., Ida, T., Yokota, M. & Yamashita, K. (2006). Surface shape measurement by phase-shifting digital holography with a wavelength shift, *Applied Optics* 45(29): 7610–7616.

URL: *http://www.ncbi.nlm.nih.gov/entrez/query.fcgi?dispmax=50&DB=pubmed&term=*
Surface+shape+measurement+by+phase-shifting+digital+holography

Yamaguchi, I., Matsumura, T. & Kato, J.-i. (2002). Phase-shifting color digital holography,
Optics Letters 27(13): 1108.
URL: *http://ol.osa.org/abstract.cfm?URI=ol-27-13-1108*

Yonemura, M. (1985). Wavelength-change characteristics of semiconductor lasers and their
application to holographic contouring, *Optics L etters* 10: 1–3.
URL: *http://ol.osa.org/abstract.cfm?id=8352*

Yu, L. & Kim, M. K. (2006). Pixel resolution control in numerical reconstruction of digital
holography, *Optics Letters* 31(7): 897.
URL: *http://ol.osa.org/abstract.cfm?URI=ol-31-7-897*

Zhang, F., Yamaguchi, I. & Yaroslavsky, L. P. (2004). Algorithm for reconstruction of digital
holograms with adjustable magnification, *Optics Letters* 29(14): 1668.
URL: *http://ol.osa.org/abstract.cfm?URI=ol-29-14-1668*

Advanced Holography - Metrology and Imaging

Edited by Dr Izabela Naydenova

Advanced Holography - Metrology and Imaging covers digital holographic microscopy and interferometry, including interferometry in the infra red. Other topics include synthetic imaging, the use of reflective spatial light modulators for writing dynamic holograms and image display using holographic screens. Holography is discussed as a vehicle for artistic expression and the use of software for the acquisition of skills in optics and holography is also presented. Each chapter provides a comprehensive introduction to a specific topic, with a survey of developments to date.

How to reference

In order to correctly reference this scholarly work, feel free to copy and paste the following:

Atsushi Wada (2011). Multiple-Wavelength Holographic Interferometry with Tunable Laser Diodes, Advanced Holography - Metrology and Imaging, Dr Izabela Naydenova (Ed.), ISBN: 978-953-307-729-1, InTech, Available from: http://www.intechopen.com/books/advanced-holography-metrology-and-imaging/multiple-wavelength-holographic-interferometry-with-tunable-laser-diodes

INTECH
open science | open minds